Cannabinoid receptor 2-selective agonist JWH015 attenuates bone cancer pain through the amelioration of impaired autophagy flux induced by inflammatory mediators in the spinal cord

YANTING MAO*, YULIN HUANG*, YING ZHANG, CHENCHEN WANG, HAO WU, XINYU TIAN, YUE LIU, BAILING HOU, YING LIANG, HUI RONG, XIAOPING GU and ZHENGLIANG MA

Department of Anaesthesiology, Affiliated Drum Tower Hospital of Medical School of Nanjing University, Nanjing, Jiangsu 210008, P.R. China

Received January 14, 2019; Accepted August 16, 2019

DOI: 10.3892/mmr.2019.10772

Abstract. Bone cancer pain (BCP) is a severe complication of advanced bone cancer. Although cannabinoid receptor 2 (CB2) agonists may have an analgesic effect, the underlying mechanism remains unclear. CB2 serves a protective role in various pathological states through the activation of autophagy. Therefore, the present study aimed to determine whether the analgesic effects of the selective CB2 agonist JWH015 was mediated by the activation of autophagy in BCP. BCP was induced by the intra-femur implantation of NCTC2472 fibrosarcoma cells in C3H/HeN mice. The pain behaviors were assessed on the following postoperative days. The selective CB2 agonist JWH015 (1 and 2 μg) was intrathecally administered on day 14 following implantation. AM630 (1 μg), a CB2 antagonist, was injected 30 min before JWH015 administration. Lipopolysaccharide (LPS; 100 nM)-stimulated primary neurons were treated with JWH015 (1 μM) and AM630 (1 μM) to further verify the mechanism by which CB2 affects autophagy. The results demonstrated that autophagy flux was impaired in spinal neurons during BCP, as indicated by the increased ratio of microtubule-associated protein 1 light chain 3β (LC3B)-II/LC3B-I and increased expression of p62. Intrathecal administration of JWH015 attenuated BCP, which was accompanied by the amelioration of impaired autophagy flux (decreased LC3B-II/LC3B-I ratio and decreased p62expression). In addition, the activation of glia cells and upregulation of the glia-derived inflammatory mediators, interleukin (IL)-1β and IL-6 were suppressed by JWH015. In LPS-stimulated primary neurons, IL-1β and IL-6 were increased, and autophagy flux was impaired; whereas treatment with JWH015 decreased the expression of IL-1β and IL-6, LC3B-II/LC3B-I ratio and expression of p62. These effects were by pretreatment with the CB2-selective antagonist AM630. The results of the present study suggested that the impairment of autophagy flux was induced by glia-derived inflammatory mediators in spinal neurons. Intrathecal administration of the selective CB2 agonist JWH015 ameliorated autophagy flux through the downregulation of IL-1β and IL-6 and attenuated BCP.

Correspondence to: Professor Xiaoping Gu or Professor Zhengliang Ma, Department of Anaesthesiology, Affiliated Drum Tower Hospital of Medical School of Nanjing University, 321 Zhong Shan Road, Nanjing, Jiangsu 210008, P.R. China
E-mail: xiaopinggu@nju.edu.cn
E-mail: mazhengliang1964@nju.edu.cn

*Contributed equally

Key words: bone cancer pain, cannabinoid receptor 2, autophagy flux, glia, inflammatory mediators

Introduction

Bone cancer pain (BCP) is a severe complication of metastatic or advanced malignancy and is characterized by allodynia and hyperalgesia (1). In total, 75-90% of patients with metastatic or advanced stage cancer have chronic severe bone pain (2). BCP negatively affects the quality of life of those suffering from it and represents a substantial burden to society (3,4). Although much effort has been devoted to the study of peripheral and central nervous system (CNS) sensitizations, the mechanism of BCP has yet to be elucidated (5), and pharmacological agents with higher analgesic efficacy and fewer side effects need to be developed.

The endocannabinoid system comprises the cannabinoid receptors, corresponding ligands and enzymes that catalyze the synthesis and degradation of cannabinoids (6). Cannabinoid receptor type 1 (CB1) is highly expressed in the CNS (7), whereas the CB2 is mainly distributed in the immune system (8). Previous studies have revealed the effects of the cannabinoid signaling system on acute and chronic pain relief; for example, pharmacological studies have demonstrated that non-selective cannabinoid agonists and selective CB1 and CB2 agonists induced antinociceptive effects (9-12). However, because of the side effects, such as sedation, dependence, cognitive impairment and psychotic-like behavior, caused by CB1 agonists (13), the pain relief mechanism of CB2 agonists in cancer pain has become a key focus.

The analgesic effects of CB2 agonists have been demonstrated in a number of pain models. (14-16). Various analgesic mechanisms of CB2 agonists have been proposed but, to date, there is no definitive explanation. There is evidence that suggests a fatal role of autophagy in neuropathic pain (17,18). For example, suberanilohydroxamic acid (SAHA) was reported to attenuate neuropathic pain through the autophagy flux mediated by mTOR signaling in spinal astrocytes and neurons (19). It has also been reported that antinociception caused by caloric restriction increased autophagy in diabetic neuropathic pain (20). Previous studies have revealed that activation of CB2 by JWH015 alleviated autoimmune disease (21), protected against alcoholic liver disease (22) and exerted an antitumor effect through the activation of autophagy (23,24). Therefore, the present study aimed to determine whether the analgesic effect of the CB2 agonist JWH015 was mediated by the increased autophagy flux.

The existence of crosstalk between autophagy and inflammation has been proposed in various diseases, such as rheumatoid arthritis, systemic lupus erythematosus and cancer (25,26). Interleukin (IL)-1β and IL-6 are inflammatory mediators, and their upregulation often occurs with impaired autophagy (27,28). Based on our previous study that demonstrated that the activation of CB2 by intrathecal injection of JWH015 inhibited the activation of glial cells and downregulated the expression of IL-1β and IL-6 in rat BCP (29), it was hypothesized that autophagy flux was impaired by the increases in inflammatory mediators in BCP. However, whether the inflammatory mediator-induced impairment of autophagy flux is involved in the analgesic effects of JWH015 remains unclear.

Therefore, the present study proposed that the activation of CB2 by JWH015 may activate autophagy, which was impaired by glia-derived inflammatory mediators. The present study investigated the specific mechanism of CB2 in BCP, with a focus on its modulation of inflammation-mediated autophagy.

Materials and methods

Animals. All experiments were performed in strict accordance with the appropriate guidelines (30) and were approved by the Animal Care and Use Committee of the Medical School of Nanjing University (Nanjing, China).

For *in vivo* experiments, male C3H/HeN mice (weight, 20-25 g; age 4-6 weeks, n=141) were purchased from Vital River Experimental Animal Corporation of Beijing. In total, 6 mice were housed in one cage under a 12 h light/dark cycle at 20˚C, with a relative humidity of 55% and with free access to water and food.

For *in vitro* experiments, 14-day pregnant Sprague-Dawley rats were used to obtain the fetuses and collected the primary neuronal cells from the fetuses. Sprague-Dawley rats in the 14th day of pregnancy (weight, 300-350 g; age 6 weeks, n=3) were purchased from Qing Long Shan Dong Wu Fan Zhi Chang (Jiangsu, China, http://www.njqlsdwc.com). Rats were housed one cage per rat under a 12 h light/dark cycle at 20˚C, with a relative humidity of 55% and with free access to water and food.

Experimental design.

Experiment 1. A total of 64 mice were randomly divided into eight groups (n=8): Control group, sham group, and tumor group, pain behavioral tests were performed on the day before (baseline) and on day 4, 7,10, 14, 21 and 28 after operation. sham + vehicle group, tumor + vehicle group, tumor + JWH015 (1 μg) group, tumor + JWH015 (2 μg) group, and tumor + JWH015 (1 μg) + AM630 (2 μg) group, pain behavioral tests were performed on the day before (baseline) and at 4, 8,12, 24, 48 and 72 h after injection.

Experiment 2. A total of 20 mice were randomly divided into two groups: Sham group (n=6), and tumor group (n=24). 14 days after operation, mice in sham group were sacrificed and the lumbar spinal cord was collected for western blotting (n=3) and immunofluorescence labeling (n=3). Mice in tumor group were sacrificed on day 0 (n=3), 4 (n=3), 7 (n=3), 10 (n=3), 14 (n=3), 21 (n=3), and 28 (n=3) for western blotting. On day 14 after operation, the mice in tumor group were sacrificed for immunofluorescence labeling (n=3).

Experiment 3. A total of 36 mice were randomly divided into eight groups: Sham + vehicle group (n=6), tumor + vehicle group (n=6), sham + Baf-A1 group (n=3), tumor + Baf-A1 group, tumor + JWH015 (1 μg) group (n=3), tumor + JWH015 (2 μg) group (n=6), tumor + JWH015 (1 μg) + AM630 (2 μg) group (n=6), and tumor + JWH015 + Baf-A1 group (n=3). Mice were sacrificed at 12 h after injection in each group for western blotting (n=3). In sham + vehicle group, tumor + vehicle group, tumor + JWH015 (2 μg) group, tumor + JWH015 (1 μg) + AM630 (2 μg) group, another 3 mice were sacrificed at 12 h after injection for immunofluorescence labeling (n=3).

Experiment 4. A total of 21 mice in tumor + JWH015 (2 μg) group were randomly sacrificed at 0 (n=3), 4 (n=3), 8 (n=3), 12 (n=3), 24 (n=3), 48 (n=3), and 72 (n=3) h after injection for western blotting.

NCTC 2472 cell culture. NCTC 2472 osteolytic sarcoma cells (cat. no. 2087787; American Type Culture Collection) were cultured in NCTC 135 medium (Sigma-Aldrich; Merck KGaA) containing 10% horse serum (Gibco; Thermo Fisher Scientific, Inc.) and maintained in a 5% CO2 atmosphere at 37˚C (Thermo Forma; Thermo Fisher Scientific, Inc.).

Primary neuronal cells culture. Sprague-Dawley rats in the 14th day of pregnancy were deeply anesthetized with 2-3% isofluorane, sacrificed by cervical dislocation and the fetuses were quickly removed on embryonic day 14. The meninges and blood vessels were removed from the fetal cerebral cortices under a dissecting microscope. After cutting into 1 mm^3 pieces, cortical tissues were digested in 0.25% trypsin at 37˚C for 10 min. Supernatants were passed through a 70 μm cell strainer (Falcon; Thermo Fisher Scientific, Inc.) and centrifuged for 5 min at 168 x g at 37˚C. Cells were diluted in Neurobasal medium (Gibco; Thermo Fisher Scientific, Inc.) supplemented with 1% B27 (Gibco; Thermo Fisher Scientific, Inc.), 2 mM glutamine and 10 μl/ml penicillin/streptomycin and plated onto poly-L-lysine (Sigma-Aldrich; Merck KGaA) coated 6-well plates at a density of $1x10^6$ cells/cm^2. Cells were cultured at 37˚C in a humidified incubator containing 5% CO_2. The culture medium was changed 3 days after plating and cells were allowed to grow for 7 days before using in subsequent experiments.

BCP model. The BCP model was constructed as described by Schwei *et al* (31). Mice were anesthetized with sodium pentobarbital (50 mg/kg; i.p.) and an incision was made in the skin on the right leg and the right joint was exposed. Then a hole was drilled in the femur-plateau. Subsequently, 20 μl α-minimum essential medium (Thermo Fisher Scientific, Inc.) containing $2x10^5$ NCTC 2472 osteolytic sarcoma cells was injected into the intramedullary space of the right femur. Mice in the Sham group were injected with the isodose medium without any cells. The drilled hole was sealed with bone wax, and the wound was closed with 4-0 silk sutures (Ethicon, Inc.). Mice recovered from anesthesia on a heated blanket.

Drug treatments. For *in vivo* experiments, drugs were prepared and administered as previously described (29,32,33). The selective CB2 agonist JWH015 (Sigma-Aldrich; Merck KGaA) was dissolved in 5% DMSO corresponding to a dose of 1 μg/5 μl (50 μg/kg) or 2 μg/5 μl (100 μg/kg). The CB2-selective antagonist AM630 (Sigma-Aldrich; Merck KGaA) was dissolved in 5% DMSO corresponding to a dose of 2 μg/5 μl (100 μg/kg). Bafilomycin A1 (Baf-A1), an inhibitor of autophagosome and lysosome fusion, was dissolved in 5% DMSO corresponding to a dose of 10 nM. To avoid systemic effects on tumor cells, intrathecal administration was selected (34). Drugs were intrathecally administered at a volume of 5 μl at day 14 after the inoculation with tumor cells. To antagonize the activation of the CB2 receptor, AM630 was injected 30 min before JWH015.

For *in vitro* experiments, JWH015 and AM630 were dissolved in culture medium corresponding to a dose of 1 μM. Lipopolysaccharide (LPS) was dissolved in culture medium corresponding to a dose of 100 nM.

Pain behavioral tests. Mechanical allodynia and spontaneous pain in mice were tested prior to operation (day 0) as well as 4, 7, 10, 14, 21 and 28 days after operation in each group, and 0 (baseline), 4, 8, 12, 24, 48 and 72 h after the administration of JWH015, AM630 and vehicles. The experimenters who performed all behavioral tests were blinded to the groups.

Paw withdrawal mechanical threshold (PWMT). PWMT in the right hind paw was measured using von Frey filaments (0.16, 0.4, 0.6, 1.0, 1.4 and 2.0 g; Stoelting, USA) and the 'up-down' method as previously described (33). Mice were placed in transparent plexiglass compartments with a wire mesh bottom and allowed to acclimate for 30 min. von Frey filaments were stuck to the plantar surface, and the lowest filament stimulus strength that resulted in the paw flinching or withdrawing was regarded as the PWMT.

Number of spontaneous flinches (NSF). Mice were placed in transparent plexiglass compartments with a wire mesh bottom and allowed to acclimatize for 30 min. Subsequently, the NSF of the right hind paw in 2 min was counted; each mouse was tested five times.

Western blotting. Mice were anesthetized with pentobarbital (50 mg/kg, i.p.) and sacrificed by cervical dislocation on day 0, 4, 7, 10, 14, 21 and 28 after operation and 0, 4, 8, 12, 24, 48 and 72 h after intrathecal administration. The L3-L5 segments of the spinal cord were removed and stored at -80˚C for further study. In addition, the primary neuronal cells were collected at 0, 3, 6, 9, 12 and 24 h after LPS-stimulation, and 12 h after JWH015-treatment. Samples were homogenized in RIPA Lysis Buffer (10 μl/mg for tissue; Beyotime Institute of Biotechnology) with phenylmethyl sulfonyl fluoride and incubated on ice for 30 min, followed by centrifugation at 241 x g at 4˚C for 20 min. The supernatant of each sample was collected. Protein concentrations were determined using a BCA Protein Assay kit. Each sample of 50 μg protein was subjected to 10% SDS-PAGE and then transferred onto a PVDF membrane. The membrane was blocked with 5% BSA (Gibco; Thermo Fisher Scientific, Inc.) at room temperature for 1 h. The membranes were incubated with primary antibodies against IL-1β (1:1,000; Abcam; cat. no. ab2105), IL-6 (1:1,000; Abcam; cat. no. ab6672), LC3B (1:1,000; Cell Signaling Technology, Inc.; cat. no. 3868), p62 (1:1,000; Abcam; cat. no. ab91526) and β-actin (1:4,000; Abcam; cat. no. ab8227). The blots were subsequently incubated with a horseradish peroxidase conjugated goat anti-rabbit secondary antibody (1:10,000; EMD Millipore; cat. no. AP132P) and developed in ECL solution (Tanon Science and Technology Co., Ltd.). Images were captured using a cooled CCD system (Tanon Science and Technology Co., Ltd.) and quantified using ImageJ v1.8.0 (National Institutes of Health).

Immunofluorescence labeling. Following the administration of general anesthesia (pentobarbital, 50 mg/kg; i.p.), mice were transcardially perfused with normal saline and 4% paraformaldehyde at day 14 after operation and 12 h after JWH015 (2 μg) administration. Lumbosacral enlargements were removed and fixed in 4% paraformaldehyde for 6 h, and then dehydrated in 30% sucrose for 48-72 h at 4˚C. After they were frozen in optimal cutting temperature compound, tissues were cut into 20 μm sections with a freezing microtome. Sections were placed in PBS and sequentially blocked with 10% goat serum (Gibco; Thermo Fisher Scientific, Inc.) containing 0.3% Triton (Tanon Science and Technology Co., Ltd.) for 2 h at room temperature. Sections were then incubated with primary antibodies for glial fibrillary acidic protein (GFAP; mouse, 1:100, Cell Signaling Technology, Inc. #80788), ionized calcium-binding adaptor molecule 1 (Iba1; rabbit, 1:300, Wako, Japan), LC3B (rabbit; 1:100; Cell Signaling Technology, Inc.; cat. no. 3868), and neuronal nuclei antigen (NeuN; mouse; 1:1,000; Abcam; cat. no. ab104224) separately overnight at 4˚C. After washing with PBS, sections were incubated with Alexa 488-conjugated goat anti-rabbit (1:3,000, Thermo Fisher Scientific, Inc.; cat. no. R37116) or Alexa 594-conjugated goat anti-mouse (1:3,000; Thermo Fisher Scientific, Inc.; cat. no. R37121) secondary antibodies. The sections were mounted on glass slides, air-dried and incubated with DAPI (Abcam) for 5 min at room temperature for nuclear staining. Images were captured using a laser-scanning confocal microscope (Olympus Corporation) and the staining density was analyzed using ImageJ (National Institutes of Health).

Statistical analyses. Data are presented as the mean ± standard deviation. Results from the behavioral study were analyzed using repeated measurements ANOVA followed by Bonferroni test post-hoc test to assess differences at each time point among and with. Western blotting results were

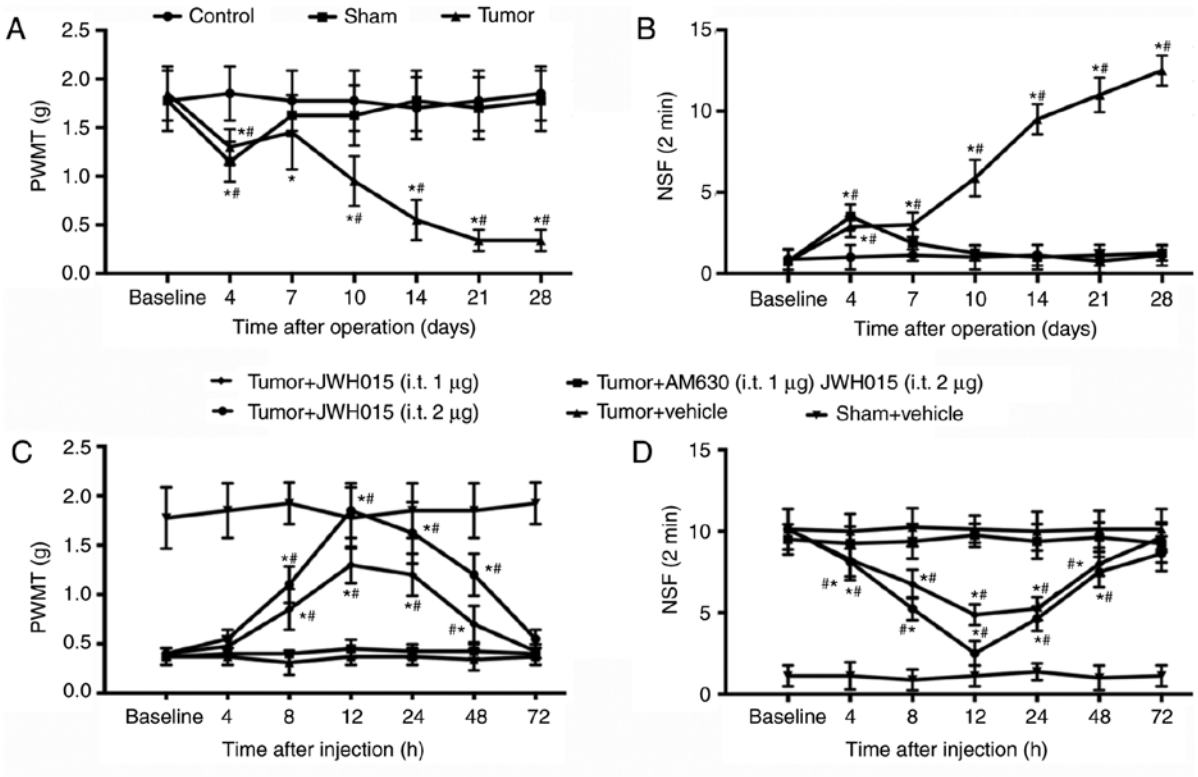

Figure 1. Intrathecal administration of JWH015 attenuates bone cancer pain. Intra-femur implantation of NCTC 2476 cells induced mechanical hypersensitivity in the ipsilateral hind paw. The (A) PWMT and (B) NSF were measured on days 0, 4, 7, 10, 14, 21 and 28 after operation in Control, Sham and Tumor group mice. JWH015 and AM630 were intrathecally injected on day 14 after the operation. (C) PWMT and (D) NSF were tested before administration (baseline, 0 h) and at 4, 8, 12, 24, 48 and 72 h after administration of JWH015. Data are expressed as the mean ± SD; n=8; *P<0.05 vs. Baseline; #P<0.05 vs. Sham at each time point. PWMT, paw withdrawal mechanical threshold; NSF, Number of spontaneous flinches.

analyzed using one-way ANOVA followed by Bonferroni test for between-group comparisons. Statistical analyses were performed using SPSS 22.0 (IBM Corporation); GraphPad Prism Version 7 (GraphPad Software, Inc.) was used to plot graphs. P<0.05 was considered to indicate a statistically significant difference.

Results

Intrathecal injection of JWH015 attenuates BCP in mice. PWMT and NSF of the right hind paw of mice were tested to monitor the progression of BCP generated by injecting NCTC 2472 osteolytic sarcoma cells into the femur. No significant differences in PWMT and NSF were observed between groups at baseline. PWMT decreased slightly (1.15±0.207 g in the Sham group; 1.30±0.185 g in the tumor group; Fig. 1A) and NSF increased (3.500±0.756 in the Sham group; 2.875±0.641 in the tumor group; Fig. 1B) on day 4 in the Sham and Tumor groups compared with the values at baseline (all P<0.05). The PWMT and NSF values recovered to near baseline level in the Sham group from day 7. In the Tumor group, PWMT recovered on day 7 and decreased starting on day 10 (0.9±0.28 g on day 10; 0.52±0.21 g on day 14; 0.34±0.11 g on days 21 and 28; P<0.05; Fig. 1A) compared with the baseline. NSF in the Tumor group remained significantly higher compared with the baseline value at days 10-28 (5.875±1.12599 on day 10; 9.5±0.92582 on day 14; 11±1.06904 on day 21 and 12.5±0.92582 on day 28; P<0.05; Fig. 1B). These results confirmed the successful establishment of the bone cancer pain model.

Activation of CB2 by intrathecal administration of JWH015 on day 14 significantly improved the pain behaviors. There were no significant differences were identified in PWMT and NSF in the Sham group following vehicle treatment. JWH015-treated mice exhibited a large increase in PWMT and a decrease in NSF in a dose-dependent manner (Fig. 1C and D, respectively). PWMT increased and NSF decreased from 8 to 48 h after administration in the Tumor + JWH015 (1 μg) group (P<0.05) and the Tumor + JWH015 (2 μg) group (P<0.05) compared with the respective baseline values. The analgesic effect of JWH015 peaked at 12 h after injection, with an increase in PWMT to 1.85±0.278 g in the Tumor + JWH015 (2 μg) group and 1.3±0.185 g in the Tumor+JWH015 (1 μg) group. However, the pain-relief effect of JWH015 was completely prevented by pretreatment with the CB2 antagonist AM630 (Fig. 1C and D).

Autophagy flux is impaired in BCP mice. There are two major autophagic marker proteins, LC3B and p62. LC3B-I is converted to LC3B-II during the formation of autophagosomes (35), whereas p62 is degraded by the autophagosome-lysosome pathway and represents the degradation level of autophagosomes (36). To determine whether autophagy flux was impaired in the spinal cord during BCP, western blotting was performed. The results indicated that LC3B-II the ratio of LC3B-II/LC3B-I were significantly increased in BCP mice at 14, 21 and 28 days after operation compared with Sham

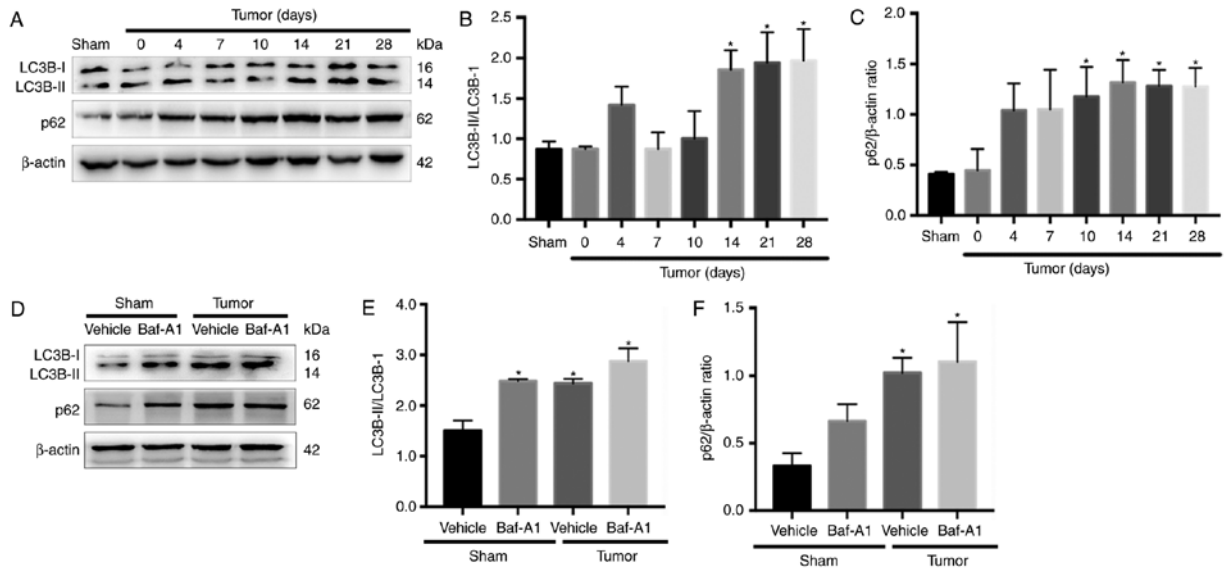

Figure 2. Autophagy flux is impaired in bone cancer pain mice. (A) Representative western blotting images of LC3BI/II and p62 protein expression in the spinal cord of mice in the Sham and Tumor groups on day 0, 4, 7, 10, 14, 21 and 28 post-operation. (B) Ratio of LC3B-II/LC3B-I and (C) quantification of p62 in the spinal cord in BCP. *P<0.05 vs. Sham group. (D) Representative blots of LC3BI/II and p62 protein expression in mice in the Sham and Tumor groups treated with or without Baf-A1 (10 nM). (E) Ratio of LC3B-II/LC3B-I and (F) quantification of p62. For all western blots, β-actin was used as a loading control. Data are expressed as the mean ± SD; n=3; *P<0.05 vs. Sham + vehicle mice. LC3B, microtubule-associated protein 1 light chain 3β.

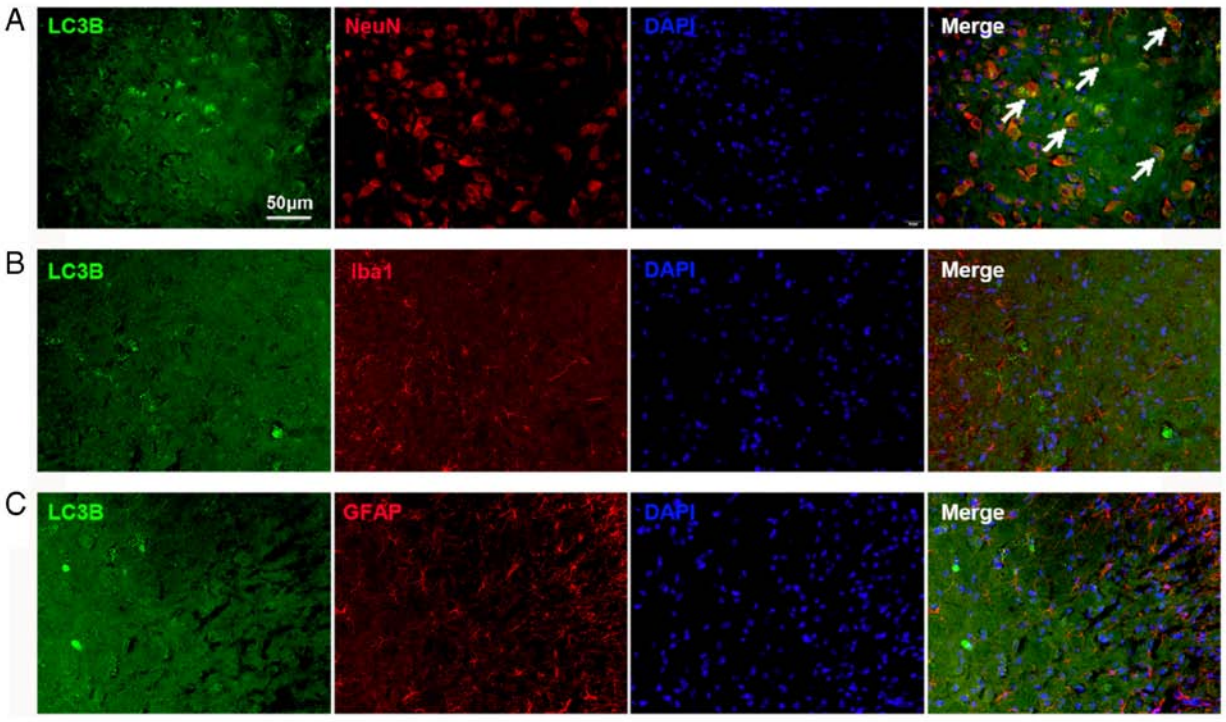

Figure 3. Autophagy flux is impaired in neurons in the spinal cord. (A-C) LC3B-immunoreactive cells (green) in the spinal cord were (A) NeuN-positive (red), (B) Iba1-negative (red), and (C) GFAP-negative (red). Scale bar, 50 μm; magnification, x400. GFAP, glial fibrillary acidic protein; Iba1, ionized calcium-binding adaptor molecule 1; LC3B, microtubule-associated protein 1 light chain 3β; NeuN, neuronal nuclei antigen.

group (Fig. 2A and B; P<0.05). In addition, the expression of p62 was significantly increased from day 10 to 28 (Fig. 2C; P<0.05).

Baf-A1 suppresses autophagosome-lysosome fusion and results in the accumulation of autophagosomes. As shown in Fig. 2D-F, intrathecal injection of 10 nM Baf-A1 increased the ratio of LC3B-II/LC3B-I and the expression of p62 in the Sham mice compared with the values in the Sham + vehicle mice (P<0.05). These results indicated that autophagy flux was impaired in BCP model mice.

Impaired autophagy flux is located in neurons in the spinal cord. The cellular localization of LC3B expression was determined using double immunofluorescence staining. The

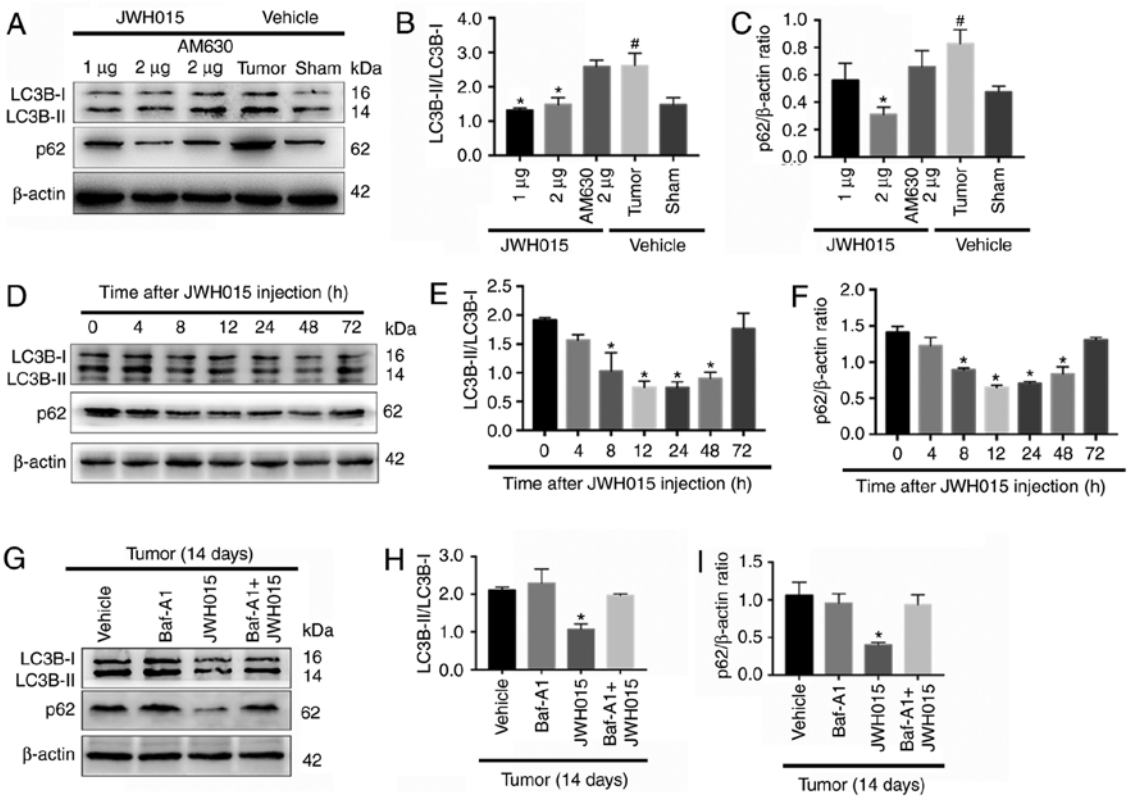

Figure 4. Intrathecal administration of JWH015 ameliorates impaired autophagy flux in bone cancer pain. (A) Representative western blotting images of LC3B and p62 in the spinal cord 12 h after treatment with JWH015. (B) Ratio of LC3B-II/LC3B-I and (C) quantification of p62 protein expression levels. #P<0.05 vs. Sham + vehicle group; *P<0.05 vs. Tumor + vehicle group. (D) Representative western blots of LC3B and p62 protein expression in the spinal cord at 0, 4, 8, 12, 24, 48 and 72 h after JWH015 (2 μg) injection. (E) Ratio of LC3B-II/LC3B-I and (F) quantification of p62. *P<0.05 vs. 0 h. (G) Representative blots of LC3B and p62 in the spinal cord with treatment of vehicle, Baf-A1 (10 nM), JWH015 (2 μg), and Baf-A1 (10 nM) + JWH015 (2 μg) in BCP mice on day 14. (H) Ratio of LC3B-II/LC3B-I. (I) Quantification of p62. *P<0.05 vs. tumor + vehicle group. For all western blots, β-actin was used as a loading control; data are expressed as the mean ± SD n=3 per group. LC3B, microtubule-associated protein 1 light chain 3β.

spinal tissues were collected on day 14 from the Tumor groups. The results demonstrated substantial LC3B expression in the spinal dorsal horn, which was mostly colocalized with NeuN, a neuronal marker (Fig. 3A). The expression of LC3B in astrocytes and microglia was also examined. No colocalization with GFAP (an astrocyte marker; Fig. 3B) and Iba1 (a microglial marker; Fig. 3C) in the spinal cord was found. These results indicated that the autophagy flux in the dorsal horn neurons was impaired in BCP.

Intrathecal administration of JWH015 ameliorates impaired autophagy flux in BCP. Based on the protective role of autophagy in pain and the relationship between autophagy and the CB2 in several diseases (19-24), the relationship between the CB2 and autophagy was involved in BCP was investigated. There were significant increase of the ratio of LC3B-II/LC3B-I and the expression of p62 in the Tumor + vehicle group compared with the Sham + vehicle group (P<0.05). Intrathecal administration of JWH015 decreased the ratio of LC3B-II/LC3B-I in the Tumor + JWH015 (1 μg) and Tumor + JWH015 (2 μg) groups, as well as decreased the expression of p62 in the tumor + JWH015 (2 μg) group, compared with the values in the Tumor + vehicle group (Fig. 4A-C; P<0.05). Pretreatment with the CB2 antagonist AM630 reversed the increased autophagy flux in the JWH015-treated mice. The protein expression levels of LC3B and p62 were also examined at different time points following JWH015 (2 μg) injection; the ratio of LC3B-II/LC3B-I and the expression of p62 decreased from 8 to 72 h after injection (Fig. 4D-F; P<0.05). In addition, the ratio of LC3B-II/LC3B-I and the expression of p62 increased in the Tumor + JWH015 (2 μg) + Baf-A1 (10 nM) group compared with the values in the Tumor + JWH015 (2 μg) group (Fig. 4G-I; P<0.05). Collectively, these results suggested that JWH015 ameliorated the impaired autophagy flux in BCP.

Intrathecal injection of JWH015 inhibits the activation of astrocytes and microglia, and downregulates IL-1β and IL-6 in BCP mice. Although the results aforementioned demonstrated the involvement of CB2-mediated autophagy flux in BCP, the mechanism by which CB2 affected autophagy was not clarified. Accumulating evidence has indicated the role of inflammation as the bridge between the CB2 and autophagy (21,22). Thus, whether the amelioration of autophagy flux by JWH015 was mediated by the modulation of inflammation was determined.

Glial cell-derived pro-inflammatory mediators, such as IL-1β and IL-6, have been reported to play key roles in the pathophysiology of pain (29). Increases in the staining density of GFAP (P<0.05) and Iba1 (P<0.05) were observed on day 14 after operation in BCP mice compared with the levels in the Sham mice (Fig. 5A). Western blotting revealed the significantly increased expression levels of IL-1β on days 4, 14, 21 and 28 (Fig. 6A and B; P<0.05) and of IL-6 on day 14 (Fig. 6A and B;

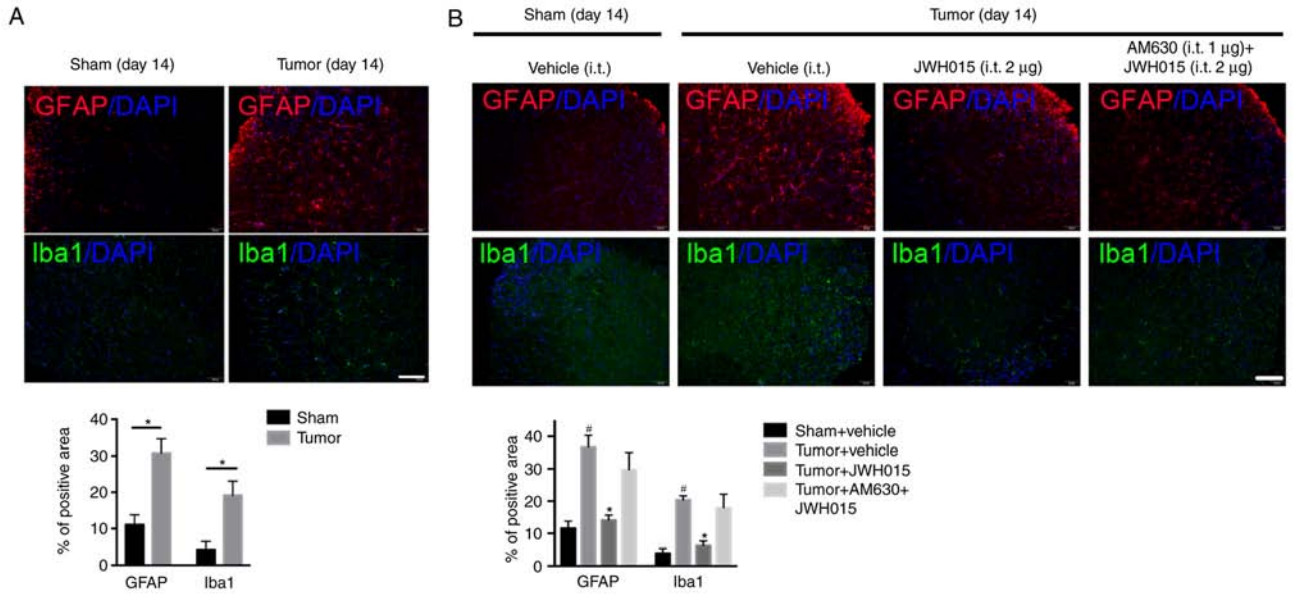

Figure 5. Intrathecal administration of JWH015 inhibits activation of astrocytes and microglia induced by bone cancer pain. (A) Images and quantification of immunostaining for GFAP (red) and Iba1 (green) in lumbar spinal dorsal horn were captured on day 14 after operation in mice in the Sham and Tumor groups. n=3; *P<0.05 vs. Sham. (B) Effects of JWH015 on glial cells are shown by immunostaining and quantification of GFAP (red) and Iba1 (green) in mice in the Sham + vehicle, Tumor + vehicle, Tumor + JWH015 (2 μg) and Tumor + AM630 (1 μg) + JWH015 (2 μg) groups at 12 h after treatment. #P<0.05 vs. Sham + vehicle group; *P<0.05 vs. Tumor + vehicle group; n=3 per group. Scale bar, 50 μm; magnification, x 200. GFAP, glial fibrillary acidic protein; Iba1, ionized calcium binding adaptor molecule 1.

P<0.05) in the spinal cord in BCP mice compared with the levels in the Sham mice.

Intrathecal administration of JWH015 at a dosage of 2 μg decreased the staining density of GFAP and Iba1 at 12 h after treatment (Fig. 5B; P<0.05) compared with the values in the Tumor + vehicle group. Compared with the values in the Tumor + vehicle group, intrathecal injection of 1 and 2 μg JWH015 significantly lowered the protein expression levels of IL-1β and IL-6 (Fig. 6C and D; P<0.05). The expression of IL-1β and IL-6 decreased between 8 and 72 h after JWH015 (2 μg) injection (Fig. 6E and F, P<0.05). However, the suppressive effect of JWH015 was completely prevented by pretreatment with AM630 (Fig. 6C and D; P>0.05).

In summary, the activation of CB2 by the intrathecal administration of JWH015 inhibited the activation of glial cells, and downregulated glial cell-derived IL-1β and IL-6, and this may be the underlying mechanism by which autophagy flux was ameliorated.

Amelioration of impaired autophagy flux in LPS-stimulated primary neurons by JWH015 is mediated by the downregulation of IL-1β and IL-6. Previous studies have reported the increased expression of IL-1β and IL-6 following LPS-stimulation in various cells (37,38). Therefore, LPS-stimulated primary neurons were used as an *in vitro* model to further explore the role of IL-1β and IL-6 in the activation of autophagy by JWH015. Primary neurons were stimulated with LPS (100 nM) for 0, 3, 6, 9, 12 or 24 h. Western blotting revealed significantly increased protein expression levels of IL-1β and IL-6 in primary neurons at 9, 12 and 24 h after LPS stimulation, compared with untreated Control cells (Fig. 7A and B; P<0.05), which indicated an inflammatory environment induced by LPS. IL-1β and IL-6 were upregulated over time following LPS stimulation, along with increases in the ratio of LC3B-II/LC3B-I and expression levels of p62 at 9, 12 and 24 h after stimulation (Fig. 7C and D; P<0.05), which indicated the impairment of autophagy flux induced by the LPS-mediated production of IL-1β and IL-6 in primary neurons. Treatment with JWH015 at a dosage of 1 μM for 12 h in LPS stimulated-primary neurons significantly reduced IL-1β and IL-6 expression levels (Fig. 7E and F; P<0.05). In addition, the ratio of LC3B-II/LC3B-I and the expression of p62 decreased in the JWH015-treated group (Fig. 7G and H; P<0.05). These effects could be prevented by pretreatment with AM630 as the expression of IL-1β and IL-6, the ratio of LC3B-II/LC3B-I, and the expression of p62 was increased in the LPS + JWH015 + AM630 group compared with the LPS + JWH015 group (P<0.05).

In summary, the results of the *in vitro* experiment demonstrated that the impairment of autophagy flux was induced by the production of IL-1β and IL-6 in LPS-stimulated primary neurons. JWH015 may ameliorate autophagy by the downregulation of the inflammatory mediators IL-1β and IL-6.

Discussion

BCP is common in patients with advanced cancer, and the extreme pain is difficult to completely control. The results of the present study demonstrated that autophagy flux was impaired during the progression of BCP. Intrathecal administration of the selective CB2 agonist JWH015 alleviated BCP through the amelioration of impaired autophagy flux in spinal neurons. The production of IL-1β and IL-6 in LPS-stimulated primary neurons impaired autophagy, and treatment with JWH015 reversed the impaired autophagy by downregulating IL-1β and IL-6 expression levels. The results indicated a potential

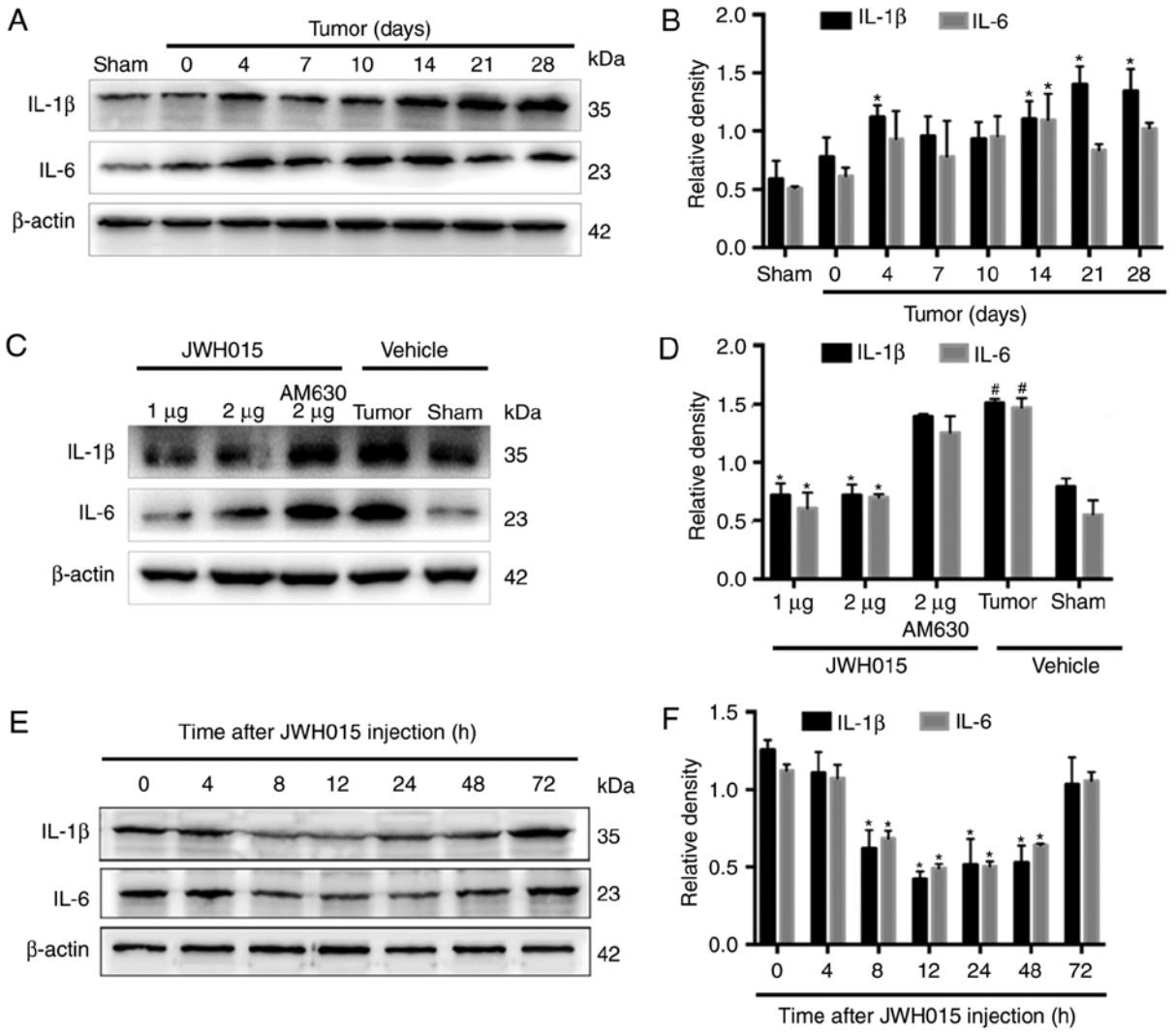

Figure 6. Intrathecal administration of JWH015 downregulated the expression of pro-inflammatory mediators IL-1β and IL-6. (A) Representative western blotting images and (B) quantification of IL-1β and IL-6 protein expression in the spinal cord in Sham and Tumor mice on day 0, 4, 7, 10, 14, 21 and 28 after the operation. *P<0.05 vs. Sham. (C) Representative western blots and (D) quantification of IL-1β and IL-6 expression in the spinal cord 12 h after the treatment of JWH015. #P<0.05 vs. Sham + vehicle group; *P<0.05 vs. Tumor + vehicle. (E) Representative blots and (F) quantification of IL-1β and IL-6 in the spinal cord at 0, 4, 8, 12, 24, 48 and 72 h after JWH015 (2 μg) injection. *P<0.05 vs. 0 h. For all blots, β-actin was used as a loading control; data are expressed as the mean ± SD; n=3. IL, interleukin.

mechanism by which the CB2 affects pain relief. Activation of the CB2 by JWH015 alleviated hyperalgesia by ameliorating the impaired autophagy induced by glia-derived inflammatory mediators in spinal neurons.

BCP remains a clinically challenging problem (39,40). Its etiology and mechanisms are complex and poorly elucidated. The current therapeutic options for BCP are not very effective and have many unresolvable side effects (41). The endocannabinoid system serves important roles in pain states, and the analgesic properties of cannabinoid receptor agonists have been extensively described (9-12). The present study verified the pain relief effect of the intrathecal administration of the CB2-selective agonist JWH015 on tumor-evoked mechanical hyperalgesia, which was similar to results reported in our previous studies (29,32,33). CB2 agonists have been shown to exert analgesic effects in various models of pain, such as inflammatory pain (42), neuropathic pain (15) and BCP. Our previous studies indicated that the CB2 could attenuate bone cancer pain via the modification of N-methyl D-aspartate receptor subtype 2B (NR2B; a subunit of NMDAR) (33), G-protein coupled receptor kinase 2 (32), inflammatory cytokines, and glial cells (29). Other studies have reported that CB2 could modulate the NACHT, LRR and PYD domains-containing protein 3 (NLRP3) inflammasome (14) and microglial phenotype (43) in different models of pain relief. These results suggested that the CB2 may induce analgesic effects through various pathways; however, little attention has been given to autophagy.

Autophagy, a cellular self-digestive process (44), is associated with several diseases, such as cancers and neurodegenerative and inflammation diseases (45,46). Autophagy has been proposed to serve a role in pain, and the impairment of autophagy has been reported in neuropathic pain (47). Metformin was demonstrated to relieve neuropathic pain through autophagy flux stimulation (48). Moreover, impaired autophagy in GABAergic interneurons was found in neuropathic pain (49). In the present study, the ratio of LC3B-II/LC3B-I

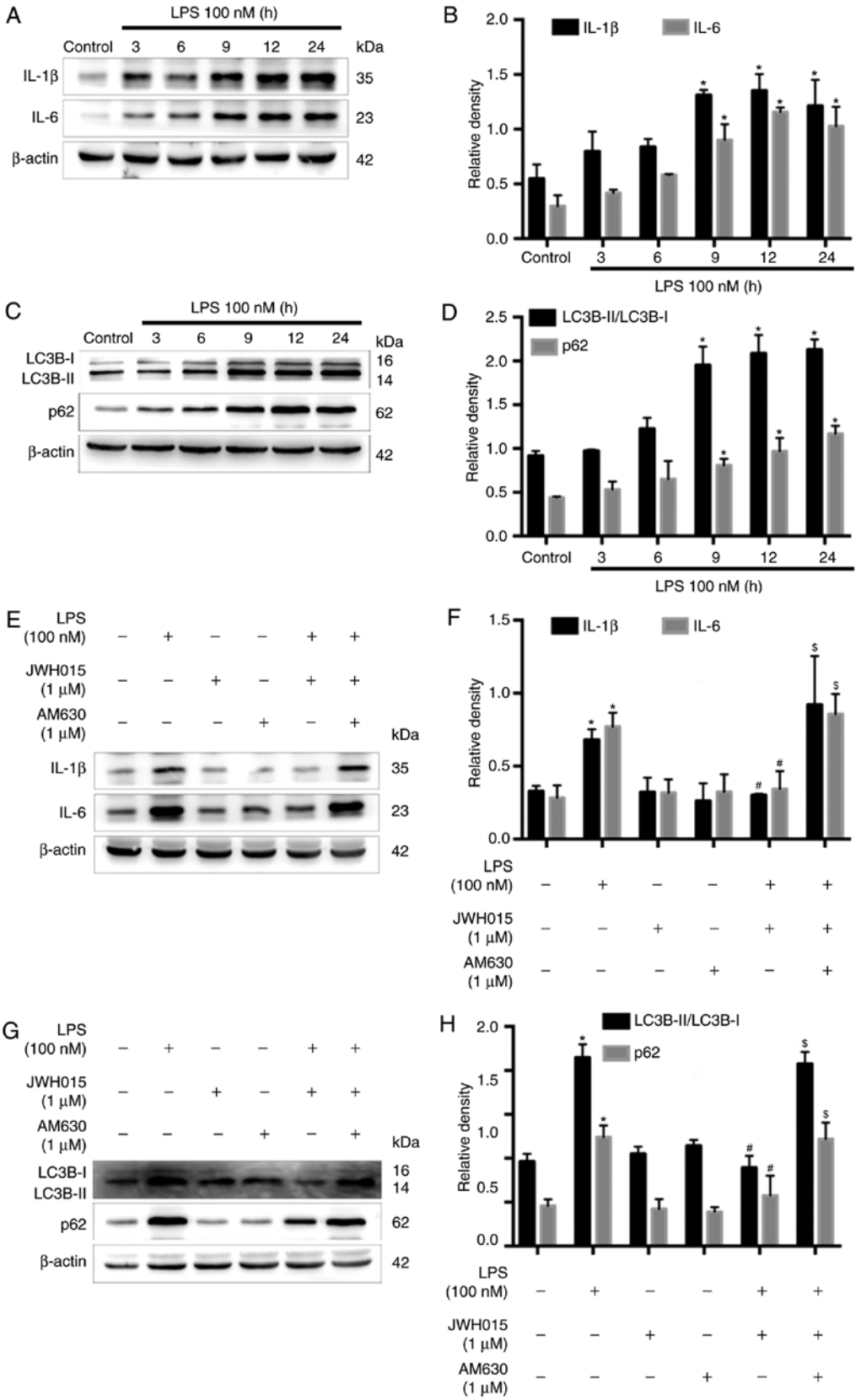

Figure 7. Effects of JWH015 on inflammatory factors and autophagy in primary neurons. Primary neurons were stimulated with LPS (100 nM) for 0, 3, 6, 9, 12 and 24 h. (A) Western blotting demonstrated the upregulation of IL-1β and IL-6 after LPS-stimulation. (B) Quantification of IL-1β and IL-6 in the primary neurons after LPS-stimulation. *P<0.05 vs. Control (0 h). (C) Increased ratio of LC3B-II/LC3B-I and increased expression of p62 in LPS-stimulated primary neurons. (D) Quantification of LC3B-II/LC3B-I and p62. *P<0.05 vs. Control (0 h). (E-H) Primary neurons were treated with JWH015 (1 μM) and AM630 (1 μM) for 12 h. (E) Inhibition of IL-1β and IL-6 after treatment with JWH015 in LPS stimulated-primary neurons. (F) Quantification of IL-1β and IL-6 in different groups. *P<0.05 vs. control group; #P<0.05 vs. LPS group; $P<0.05 vs. LPS + JWH015 group. (G) Decreased ratio of LC3B-II/LC3B-I and decreased expression of p62 after treatment with JWH015 in LPS-stimulated primary neurons. (H) Quantification of LC3B-II/LC3B-I and p62 in different groups. *P<0.05 vs. control group; #P<0.05 vs. LPS group; $P<0.05 vs. LPS + JWH015 group. In all western blots, β-actin was used as a loading control; data are expressed as the mean ± SD; n=3. IL, interleukin; LC3B, microtubule-associated protein 1 light chain 3β; LPS, lipopolysaccharide.

and the expression of p62 increased, which indicated decreased formation of autophagosomes and degradation of the autophagosome-lysosome pathway. Baf-A1, an inhibitor of autophagosome and lysosome fusion, induced an increase in the ratio of LC3B-II/LC3B-I in the Sham mice and exacerbated the increase in the ratio of LC3B-II/LC3B-I in the Tumor mice. These results provided further evidence of the impaired autophagy flux in BCP. A relationship between the CB2 and autophagy has been proposed in various diseases (21,22). The CB2-selective agonist JWH015 is capable of inhibiting tumor cell growth through the stimulation of autophagy (23,24). Thus, the expression levels of autophagy proteins in BCP mice treated with JWH015 were investigated. A decrease in the ratio of LC3B-II/LC3B-I and the downregulation of p62 in neurons were found in JWH015-treated mice compared with the levels in vehicle-treated mice. The increase in autophagy flux together with the attenuation of tumor-evoked mechanical hyperalgesia indicated that autophagy may serve an important role in the analgesic mechanism of CB2.

Several mechanisms for the modulation of autophagy by the CB2 have been proposed, mainly focusing on inflammation (50,21,20). For example, cannabinoids can inhibit energetic metabolism and induce AMPK-dependent autophagy in pancreatic cancer cells (50). Activation of CB2 by JWH133 was reported to inhibit hepatic inflammation and activate autophagy in macrophages in alcoholic liver disease (21). Inhibition of NLRP3 inflammasomes and activation of autophagy were found in HU308 (a specific agonist of CB2R)-stimulated BV2 cells (20). Crosstalk between autophagy and inflammation is involved in many pathological conditions. For example, autophagy suppresses inflammation in kidney diseases (51) and environmental ultrafine particulate matter (PM)-induced airway epithelial injury (52). Only limited studies have focused on the effect of inflammation on autophagy (27,28). The present study explored the possible mechanism by which glia-derived pro-inflammatory mediators induced autophagy in BCP. It was demonstrated that the impairment of autophagy in BCP mainly occurred in spinal neurons. Thus, the mechanism of inflammation-induced autophagy in primary neurons was investigated. After stimulation by LPS, the expression of IL-1β and IL-6 was increased and autophagy was impaired in primary neurons. These results suggested that stimulation by inflammatory mediators may impair autophagy in neurons. Treatment with JWH015 increased the expression of autophagy-related proteins and downregulated IL-1β and IL-6, which further verified the results of the *in vivo* experiments.

In conclusion, the results of the present study indicated that intrathecal administration of the selective CB2 agonist JWH015 alleviated BCP and that the amelioration of impaired neuronal autophagy mediated by the downregulation of glia-derived IL-1β and IL-6 may underlie this pain-relief effect. This was a preliminary study and further studies are required to elucidate the function of autophagy in different cell types.

Acknowledgements

Not applicable.

Funding

The present study was supported by The National Natural Science Foundation of China (grant. nos. 81471129, 81671087, 81500954, 81701102 and 81771142) and a grants from The Department of Health of Jiangsu Province of China (grant. nos. XK101140 and RC2011006).

Availability of data and materials

All data generated or analyzed during the present study are included in this published article.

Authors' contributions

YM, ZM and XG conceived and designed the experiments. YM, YH, YZ and CW carried out all experiments. YM, YH, HW, XT, YuL, BH, YiL and HR helped conduct the experiments and analyzed the data. All authors read and approved the final manuscript.

Ethics approval and consent to participate

All animal experiments conformed with the Regulation of Animal Care Management of the Ministry of Public Health, People's Republic of China and were approved by the Ethical Committee of the Medical School of Nanjing University (Nanjing, China).

Patient consent for publication

Not applicable.

Competing interests

The authors declare that they have no competing interests.

References

1. Mantyh P: Bone cancer pain: Causes, consequences, and therapeutic opportunities. Pain 154 (Suppl 1): S54-S62, 2013.
2. Mantyh PW: Cancer pain and its impact on diagnosis, survival and quality of life. Nat Rev Neurosci 7: 797-809, 2006.
3. Honore P, Luger NM, Sabino MA, Schwei MJ, Rogers SD, Mach DB, O'keefe PF, Ramnaraine ML, Clohisy DR and Mantyh PW: Osteoprotegerin blocks bone cancer-induced skeletal destruction, skeletal pain and pain-related neurochemical reorganization of the spinal cord. Nat Med 6: 521-528, 2000.
4. Miller K, Steger GG, Niepel D and Luftner D: Harnessing the potential of therapeutic agents to safeguard bone health in prostate cancer. Prostate Cancer Prostatic Dis 21: 461-472, 2018.
5. Ji RR, Xu ZZ and Gao YJ: Emerging targets in neuroinflammation-driven chronic pain. Nat Rev Drug Discov 13: 533-548, 2014.
6. Ligresti A, De Petrocellis L and Di Marzo V: From phytocannabinoids to cannabinoid receptors and endocannabinoids: Pleiotropic physiological and pathological roles through complex pharmacology. Physiol Rev 96: 1593-1659, 2016.
7. Kendall DA and Yudowski GA: Cannabinoid receptors in the central nervous system: Their signaling and roles in disease. Front Cell Neurosci 10: 294, 2016.
8. Devane WA, Dysarz FA III, Johnson MR, Melvin LS and Howlett AC: Determination and characterization of a cannabinoid receptor in rat brain. Mol Pharmacol 34: 605-613, 1988.
9. Pernia-Andrade AJ, Kato A, Witschi R, Nyilas R, Katona I, Freund TF, Watanabe M, Filitz J, Koppert W, Schüttler J, *et al*: Spinal endocannabinoids and CB1 receptors mediate C-fiber-induced heterosynaptic pain sensitization. Science 325: 760-764, 2009.

10. Racz I, Nadal X, Alferink J, Baños JE, Rehnelt J, Martín M, Pintado B, Gutierrez-Adan A, Sanguino E, Manzanares J, *et al*: Crucial role of CB(2) cannabinoid receptor in the regulation of central immune responses during neuropathic pain. J Neurosci 28: 12125-12135, 2008.
11. Pertwee RG: Targeting the endocannabinoid system with cannabinoid receptor agonists: Pharmacological strategies and therapeutic possibilities. Philos Trans R Soc Lond B Biol Sci 367: 3353-3363, 2012.
12. Fernandez-Ruiz J, Romero J, Velasco G, Tolon RM, Ramos JA and Guzman M: Cannabinoid CB2 receptor: A new target for controlling neural cell survival? Trends Pharmacol Sci 28: 39-45, 2007.
13. Kalant H: Adverse effects of cannabis on health: An update of the literature since 1996. Prog Neuropsychopharmacol Biol Psychiatry 28: 849-863, 2004.
14. Gao F, Xiang HC, Li HP, Jia M, Pan XL, Pan HL and Li M: Electroacupuncture inhibits NLRP3 inflammasome activation through CB2 receptors in inflammatory pain. Brain Behav Immun 67: 91-100, 2018.
15. Niu J, Huang D, Zhou R, Yue M, Xu T, Yang J, He L, Tian H, Liu X and Zeng J: Activation of dorsal horn cannabinoid CB2 receptor suppresses the expression of P2Y12 and P2Y13 receptors in neuropathic pain rats. J Neuroinflammation 14: 185, 2017.
16. La Porta C, Bura SA, Aracil-Fernandez A, Manzanares J and Maldonado R: Role of CB1 and CB2 cannabinoid receptors in the development of joint pain induced by monosodium iodoacetate. Pain 154: 160-174, 2013.
17. Li AL, Lin X, Dhopeshwarkar AS, Thomaz AC, Carey LM, Liu Y, Nikas SP, Makriyannis A, Mackie K and Hohmann AG: Cannabinoid CB2 Agonist AM1710 differentially suppresses distinct pathological pain states and attenuates morphine tolerance and withdrawal. Mol Pharmacol 95: 155-168, 2019.
18. Wu J, Hocevar M, Bie B, Foss JF and Naguib M: Cannabinoid Type 2 receptor system modulates Paclitaxel-induced microglial dysregulation and central sensitization in rats. J Pain 20: 501-514, 2018.
19. Feng XL, Deng HB, Wang ZG, Wu Y, Ke JJ and Feng XB: Suberoylanilide hydroxamic acid triggers autophagy by influencing the mTOR pathway in the spinal dorsal horn in a rat neuropathic pain model. Neurochem Res 44: 450-464, 2018.
20. Coccurello R, Nazio F, Rossi C, De Angelis F, Vacca V, Giacovazzo G, Procacci P, Magnaghi V, Ciavardelli D and Marinelli S: Effects of caloric restriction on neuropathic pain, peripheral nerve degeneration and inflammation in normometabolic and autophagy defective prediabetic Ambra1 mice. PLoS One 13: e0208596, 2018.
21. Shao BZ, Wei W, Ke P, Xu ZQ, Zhou JX and Liu C: Activating cannabinoid receptor 2 alleviates pathogenesis of experimental autoimmune encephalomyelitis via activation of autophagy and inhibiting NLRP3 inflammasome. CNS Neurosci Ther 20: 1021-1028, 2014.
22. Denaes T, Lodder J, Chobert MN, Ruiz I, Pawlotsky JM, Lotersztajn S and Teixeira-Clerc F: The Cannabinoid Receptor 2 protects against alcoholic liver disease via a macrophage autophagy-dependent pathway. Sci Rep 6: 28806, 2016.
23. Vara D, Salazar M, Olea-Herrero N, Guzman M, Velasco G and Diaz-Laviada I: Anti-tumoral action of cannabinoids on hepatocellular carcinoma: Role of AMPK-dependent activation of autophagy. Cell Death Differ 18: 1099-1111, 2011.
24. Salazar M, Carracedo A, Salanueva IJ, Hernández-Tiedra S, Lorente M, Egia A, Vázquez P, Blázquez C, Torres S, García S, *et al*: Cannabinoid action induces autophagy-mediated cell death through stimulation of ER stress in human glioma cells. J Clin Invest 119: 1359-1372, 2009.
25. Netea-Maier RT, Plantinga TS, van de Veerdonk FL, Smit JW and Netea MG: Modulation of inflammation by autophagy: Consequences for human disease. Autophagy 12: 245-260, 2016.
26. Tian R, Li Y and Yao X: PGRN suppresses inflammation and promotes autophagy in keratinocytes through the Wnt/β-Catenin signaling pathway. Inflammation 39: 1387-1394, 2016.
27. Sil S, Niu F, Tom E, Liao K, Periyasamy P and Buch S: Cocaine mediated neuroinflammation: Role of dysregulated autophagy in pericytes. Mol Neurobiol 56: 3576-3590, 2019.
28. Piippo N, Korhonen E, Hytti M, Kinnunen K, Kaarniranta K and Kauppinen A: Oxidative stress is the principal contributor to inflammasome activation in retinal pigment epithelium cells with defunct proteasomes and autophagy. Cell Physiol Biochem 49: 359-367, 2018.
29. Lu C, Liu Y, Sun B, Sun Y, Hou B, Zhang Y, Ma Z and Gu X: Intrathecal injection of JWH-015 attenuates bone cancer pain via time-dependent modification of pro-inflammatory cytokines expression and astrocytes activity in spinal cord. Inflammation 38: 1880-1890, 2015.
30. Demers G, Griffin G, De Vroey G, Haywood JR, Zurlo J and Bédard M: Animal research. Harmonization of animal care and use guidance. Science 312: 700-701, 2006.
31. Schwei MJ, Honore P, Rogers SD, Salak-Johnson JL, Finke MP, Ramnaraine ML, Clohisy DR and Mantyh PW: Neurochemical and cellular reorganization of the spinal cord in a murine model of bone cancer pain. J Neurosci 19: 10886-10897, 1999.
32. Lu C, Shi L, Sun B, Zhang Y, Hou B, Sun Y, Ma Z and Gu X: A single intrathecal or intraperitoneal injection of CB2 receptor agonist attenuates bone cancer pain and induces a time-dependent modification of GRK2. Cell Mol Neurobiol 37: 101-109, 2017.
33. Gu X, Mei F, Liu Y, Zhang R, Zhang J and Ma Z: Intrathecal administration of the cannabinoid 2 receptor agonist JWH015 can attenuate cancer pain and decrease mRNA expression of the 2B subunit of N-methyl-D-aspartic acid. Anesth Analg 113: 405-411, 2011.
34. Hylden JL and Wilcox GL: Intrathecal morphine in mice: A new technique. Eur J Pharmacol 67: 313-316, 1980.
35. Mizushima N and Klionsky DJ: Protein turnover via autophagy: Implications for metabolism. Annu Rev Nutr 27: 19-40, 2007.
36. Bjorkoy G, Lamark T, Brech A, Outzen H, Perander M, Overvatn A, Stenmark H and Johansen T: p62/SQSTM1 forms protein aggregates degraded by autophagy and has a protective effect on huntingtin-induced cell death. J Cell Biol 171: 603-614, 2005.
37. Hu Y, Li G, Zhang Y, Liu N, Zhang P, Pan C, Nie H, Li Q and Tang Z: Upregulated TSG-6 expression in ADSCs inhibits the BV2 Microglia-mediated inflammatory response. Biomed Res Int 2018: 7239181, 2018.
38. Ye J, Guan M, Lu Y, Zhang D, Li C and Zhou C: Arbutin attenuates LPS-induced lung injury via Sirt1/Nrf2/NF-kappaBp65 pathway. Pulm Pharmacol Ther 54: 53-59, 2019.
39. Rubens RD: Bone metastases-the clinical problem. Eur J Cancer 34: 210-213, 1998.
40. Weilbaecher KN, Guise TA and McCauley LK: Cancer to bone: A fatal attraction. Nat Rev Cancer 11: 411-425, 2011.
41. Sturge J, Caley MP and Waxman J: Bone metastasis in prostate cancer: Emerging therapeutic strategies. Nat Rev Clin Oncol 8: 357-368, 2011.
42. Li MH, Suchland KL and Ingram SL: Compensatory Activation of cannabinoid CB2 receptor inhibition of GABA release in the rostral ventromedial medulla in inflammatory pain. J Neurosci 37: 626-636, 2017.
43. Luongo L, Palazzo E, Tambaro S, Giordano C, Gatta L, Scafuro MA, Rossi FS, Lazzari P, Pani L, de Novellis V, *et al*: 1-(2',4'-dichlorophenyl)-6-methyl-N-cyclohexylamine-1,4-dihydroindeno[1,2-c]pyrazole-3-carboxamide, a novel CB2 agonist, alleviates neuropathic pain through functional microglial changes in mice. Neurobiol Dis 37: 177-185, 2010.
44. Glick D, Barth S and Macleod KF: Autophagy: Cellular and molecular mechanisms. J Pathol 221: 3-12, 2010.
45. Kumar D, Shankar S and Srivastava RK: Rottlerin-induced autophagy leads to the apoptosis in breast cancer stem cells: Molecular mechanisms. Mol Cancer 12: 171, 2013.
46. Deretic V, Saitoh T and Akira S: Autophagy in infection, inflammation and immunity. Nat Rev Immunol 13: 722-737, 2013.
47. Piao Y, Gwon DH, Kang DW, Hwang TW, Shin N, Kwon HH, Shin HJ, Yin Y, Kim JJ, Hong J, *et al*: TLR4-mediated autophagic impairment contributes to neuropathic pain in chronic constriction injury mice. Mol Brain 11: 11, 2018.
48. Weng W, Yao C, Poonit K, Zhou X, Sun C, Zhang F and Yan H: Metformin relieves neuropathic pain after spinal nerve ligation via autophagy flux stimulation. J Cell Mol Med 23: 1313-1324, 2019.
49. Yin Y, Yi MH and Kim DW: Impaired autophagy of GABAergic interneurons in neuropathic pain. Pain Res Manag 2018: 9185368, 2018.
50. Dando I, Donadelli M, Costanzo C, Dalla Pozza E, D'Alessandro A, Zolla L and Palmieri M: Cannabinoids inhibit energetic metabolism and induce AMPK-dependent autophagy in pancreatic cancer cells. Cell Death Dis 4: e664, 2013.
51. Kimura T, Isaka Y and Yoshimori T: Autophagy and kidney inflammation. Autophagy 13: 997-1003, 2017.
52. Chen ZH, Wu YF, Wang PL, Wu YP, Li ZY, Zhao Y, Zhou JS, Zhu C, Cao C, Mao YY, *et al*: Autophagy is essential for ultrafine particle-induced inflammation and mucus hyperproduction in airway epithelium. Autophagy 12: 297-311, 2016.